

Charged Higgs phenomenology in the flipped two Higgs doublet model

Heather E. Logan^{1,*} and Deanna MacLennan¹

¹*Ottawa-Carleton Institute for Physics,
Carleton University, Ottawa K1S 5B6 Canada*

(Dated: October 29, 2018)

Abstract

We study the phenomenology of the charged Higgs boson in the “flipped” two Higgs doublet model, in which one doublet gives mass to up-type quarks and charged leptons and the other gives mass to down-type quarks. We present the charged Higgs branching ratios and summarize the indirect constraints. We extrapolate existing LEP searches for H^+H^- and Tevatron searches for $t\bar{t}$ with $t \rightarrow H^+b$ into the flipped model and extract constraints on M_{H^+} and the parameter $\tan\beta$. We finish by reviewing existing LHC charged Higgs searches and suggest that the LHC reach in this model could be extended for charged Higgs masses below the $t\bar{b}$ threshold by considering $t\bar{t}$ with $t \rightarrow H^+b$ and $H^+ \rightarrow q\bar{q}'$, as has been used in Tevatron searches.

*Electronic address: logan@physics.carleton.ca

Model	Type I	Type II	Lepton-specific	Flipped
Φ_1	–	d, ℓ	ℓ	d
Φ_2	u, d, ℓ	u	u, d	u, ℓ

TABLE I: The four possible assignments of fermion couplings to two Higgs doublets that satisfy natural flavor conservation. Here u , d , and ℓ represent up- and down-type quarks and charged leptons, respectively.

I. INTRODUCTION

The Standard Model (SM) of electroweak interactions [1] has been stringently tested over the past twenty years and is in excellent agreement with all collider data. The dynamics of electroweak symmetry breaking, however, remain unknown. While the simplest possibility is the minimal Higgs mechanism [2] implemented with a single scalar SU(2) doublet, many extensions of the SM enlarge the Higgs sector to contain additional scalars.

Extensions of the SM Higgs sector are tightly constrained by two pieces of data: (i) the rho parameter, $\rho \equiv M_W^2/M_Z^2 \cos^2 \theta_W \simeq 1$, where M_W (M_Z) is the W^\pm (Z) boson mass and θ_W is the weak mixing angle; and (ii) the absence of large flavor-changing neutral currents. The first of these constraints is automatically satisfied by Higgs sectors that contain only SU(2) doublets (with the possible addition of singlets). The simplest such model that contains a charged Higgs boson is a two-Higgs-doublet model (2HDM). The second of these constraints is automatically satisfied by models in which the masses of fermions with a common electric charge are generated through couplings to exactly one Higgs doublet; this is known as natural flavor conservation [3] and prevents the appearance of tree-level flavor-changing neutral Higgs interactions.¹

Imposing natural flavor conservation, there are four different ways [9, 10] to couple the SM fermions to two Higgs doublets, as summarized in Table I.² Each of these four coupling assignments gives rise to a different phenomenology for the charged Higgs boson H^\pm . In

¹ The 2HDM without natural flavor conservation is known as the Type III model [4]; for a review of its phenomenology see Ref. [5]. In this model the basis chosen for the two Higgs doublets is somewhat arbitrary; basis-independent methods have been developed in Refs. [6, 7]. The flavor-conserving limit of the Type III model, in which the two Yukawa matrices for each fermion type are required to be diagonal in the same fermion mixing basis, has been developed in Refs. [8] under the name minimal flavor violation.

² We ignore neutrino masses.

each case, the charged Higgs couplings can be parameterized in terms of the free parameter $\tan\beta \equiv \langle\Phi_2^0\rangle/\langle\Phi_1^0\rangle$.

The Type-I and -II 2HDMs have been studied extensively. In particular, the Type-II 2HDM [11–14], in which one doublet generates the masses of up-type quarks while the other generates the masses of down-type quarks and charged leptons, arises naturally in supersymmetric models; this model has dominated 2HDM collider studies. The Type-I 2HDM [15, 16], in which one doublet generates the masses of all quarks and leptons while the other contributes only to the W^\pm and Z boson masses, has also been widely considered, particularly in the context of indirect constraints. More recently, the lepton-specific 2HDM [9, 10] has received attention because of its possible role in neutrino mass [17] and dark matter [18] models and its potential to modify the signatures of the SM-like Higgs at the CERN Large Hadron Collider (LHC) [19]. Charged Higgs phenomenology in this model has been studied in Refs. [20, 21].

In this paper we study the remaining model, in which one doublet $\Phi_u \equiv \Phi_2$ gives mass to up-type quarks and charged leptons and the other doublet $\Phi_d \equiv \Phi_1$ gives mass to down-type quarks. This scenario has been referred to in the literature as Model IB [9, 10], Model III [22], Model II' [23], the flipped 2HDM [24], and the Type-Y 2HDM [20]; following Ref. [24] we will call it the flipped 2HDM. This coupling structure was first introduced in Refs. [9, 10] and its phenomenology has been studied together with that of the other three models in Refs. [20, 22–26]. The early studies in Refs. [22, 23] focused on indirect constraints while Refs. [25] and [26] considered phenomenology (mainly of the neutral Higgs bosons) at the CERN Large Electron-Positron (LEP) Collider and the LHC, respectively. Reference [24] addressed the coupling patterns of the neutral CP-even Higgs bosons. Finally, Ref. [20] presented decay branching ratios for the charged and neutral Higgs bosons.

Our aim in this paper is to provide a comprehensive study of the existing constraints and LHC search prospects for the flipped 2HDM. We begin in Sec. II with an outline of the model structure of the flipped 2HDM and the relevant Feynman rules for the charged Higgs couplings. In Sec. III we show the decay branching fractions of the charged Higgs as a function of its mass and $\tan\beta$ and compare them to those in the Type-II 2HDM. In Sec. IV we review the indirect constraints on the model, the strongest of which comes from $b \rightarrow s\gamma$ and constrains the charged Higgs mass to be above about 200–300 GeV, the same as in the Type-II 2HDM. However, a lighter charged Higgs may be possible if additional flavor-

violating physics leads to cancellations in the $b \rightarrow s\gamma$ rate. In Sec. V we thus reinterpret the existing charged Higgs limits from LEP (due to $e^+e^- \rightarrow H^+H^-$) and the Fermilab Tevatron (due to $t\bar{t}$ production with $t \rightarrow bH^+$) to provide direct search limits in the flipped model for the first time. In Sec. VI we then review existing LHC studies of charged Higgs signatures performed in the context of the Type-II 2HDM and translate them for the first time into the flipped 2HDM. We show that while the production cross sections of the charged Higgs at the LHC are identical to the corresponding modes in the Type-II 2HDM, the different decay branching fractions below the $H^+ \rightarrow tb$ threshold lead to very different signatures—in particular, the usual $\tau\nu$ decay of the charged Higgs in the Type-II model is replaced by decays to quarks ($c\bar{b}$ and $c\bar{s}$) in most of the parameter space. Above the tb threshold the decay of the charged Higgs to tb dominates in both the flipped and Type-II model and existing LHC studies of this channel carry over. Finally we summarize our conclusions in Sec. VII.

II. THE MODEL

We begin as usual with two complex SU(2)-doublet scalar fields Φ_u and Φ_d ,

$$\Phi_i = \begin{pmatrix} \phi_i^+ \\ (v_i + \phi_i^{0,r} + i\phi_i^{0,i})/\sqrt{2} \end{pmatrix}, \quad i = u, d, \quad (1)$$

where the vacuum expectation values (vevs) of the two doublets are constrained by the W mass to satisfy $v_u^2 + v_d^2 = v_{\text{SM}}^2 \simeq 246$ GeV. To enforce the desired structure of the Yukawa Lagrangian we impose a discrete symmetry under which Φ_d and the right-handed down-type quarks transform according to

$$\Phi_d \rightarrow -\Phi_d, \quad d_{Rj} \rightarrow -d_{Rj}, \quad (2)$$

while all other fields remain invariant.³ The Yukawa Lagrangian is then,

$$\mathcal{L}_{\text{Yuk}} = \sum_{i,j=1}^3 \left[y_{ij}^u \bar{u}_{Ri} \tilde{\Phi}_u^\dagger Q_{Lj} + y_{ij}^d \bar{d}_{Ri} \Phi_d^\dagger Q_{Lj} + y_{ij}^\ell \bar{\ell}_{Ri} \Phi_u^\dagger L_{Lj} \right] + \text{h.c.}, \quad (3)$$

³ In order to preserve natural flavor conservation, this discrete symmetry may be broken only by dimension-two terms in the scalar potential. We further assume CP conservation in the scalar potential.

where i, j are generation indices, $y_{ij}^{u,d,\ell}$ are 3×3 complex Yukawa coupling matrices, Q_L and L_L are the left-handed quark and lepton doublets, and the conjugate Higgs doublet $\tilde{\Phi}$ is given by

$$\tilde{\Phi}_i \equiv i\sigma_2 \Phi_i^* = \begin{pmatrix} (v_i + \phi_i^{0,r} - i\phi_i^{0,i})/\sqrt{2} \\ -\phi_i^- \end{pmatrix}. \quad (4)$$

Defining $\tan \beta \equiv v_u/v_d$, the physical charged Higgs boson is

$$H^\pm = -\sin \beta \phi_d^\pm + \cos \beta \phi_u^\pm. \quad (5)$$

The Feynman rules for charged Higgs boson couplings to fermions are then given as follows, with all particles incoming:⁴

$$\begin{aligned} H^+ \bar{u}_i d_j &: \frac{ig}{\sqrt{2}M_W} V_{ij} (\cot \beta m_{ui} P_L + \tan \beta m_{dj} P_R) \\ H^+ \bar{\nu}_i \ell_i &: \frac{ig}{\sqrt{2}M_W} \cot \beta m_{\ell i} P_R. \end{aligned} \quad (9)$$

Here V_{ij} is the CKM matrix and $P_{L,R} \equiv (1 \mp \gamma^5)/2$ are the left- and right-handed projection operators. We ignore neutrino masses and thus take ν_i as the flavor eigenstate corresponding to the charged lepton ℓ_i . In particular, the $H^+ \bar{u}d$ coupling is identical to that in the familiar Type-II 2HDM (compare Eq. 7), while the $H^+ \bar{\nu}\ell$ coupling has the opposite $\tan \beta$ dependence.

⁴ For comparison, the corresponding couplings in the Type-I 2HDM are [27]

$$\begin{aligned} H^+ \bar{u}_i d_j &: \frac{ig}{\sqrt{2}M_W} V_{ij} \cot \beta (m_{ui} P_L - m_{dj} P_R) \\ H^+ \bar{\nu}_i \ell_i &: -\frac{ig}{\sqrt{2}M_W} \cot \beta m_{\ell i} P_R, \end{aligned} \quad (6)$$

with $\tan \beta = v_2/v_1$, where v_2 is the vev of the Higgs field that couples to fermions; the other doublet is decoupled from fermions. In the Type-II 2HDM the couplings are [27]

$$\begin{aligned} H^+ \bar{u}_i d_j &: \frac{ig}{\sqrt{2}M_W} V_{ij} (\cot \beta m_{ui} P_L + \tan \beta m_{dj} P_R) \\ H^+ \bar{\nu}_i \ell_i &: \frac{ig}{\sqrt{2}M_W} \tan \beta m_{\ell i} P_R, \end{aligned} \quad (7)$$

again with $\tan \beta = v_2/v_1$; this time v_1 (v_2) is the vev of the doublet that couples to down-type quarks and charged leptons (up-type quarks). Finally, in the lepton-specific 2HDM the couplings are [22]

$$\begin{aligned} H^+ \bar{u}_i d_j &: \frac{ig}{\sqrt{2}M_W} V_{ij} \cot \beta (m_{ui} P_L - m_{dj} P_R), \\ H^+ \bar{\nu}_i \ell_i &: \frac{ig}{\sqrt{2}M_W} \tan \beta m_{\ell i} P_R, \end{aligned} \quad (8)$$

with $\tan \beta = v_q/v_\ell$, where v_q is the vev of the doublet that couples to up- and down-type quarks while v_ℓ is the vev of the doublet that couples to leptons.

The allowed range of $\tan\beta$ can be constrained by the requirement that the Yukawa couplings remain perturbative, $y_i^2/4\pi \lesssim 1$. The top quark Yukawa coupling $y_t = \sqrt{2}m_t/v_{\text{SM}} \sin\beta$ provides a lower limit on $\tan\beta$ and the bottom quark Yukawa coupling $y_b = \sqrt{2}m_b/v_{\text{SM}} \cos\beta$ provides an upper limit. Taking $m_t = 171.3$ GeV [28] and $m_b = 4.20$ GeV ($\overline{\text{MS}}$ mass [28]), we obtain

$$0.29 \lesssim \tan\beta \lesssim 150. \quad (10)$$

We will work in a range of $\tan\beta$ corresponding to more moderate values of the Yukawa couplings; for reference, we note that

$$0.49 \text{ (0.98)} \leq \tan\beta \leq 83 \text{ (41)} \quad \text{for } y_t, y_b \leq 2 \text{ (1)}. \quad (11)$$

III. CHARGED HIGGS BOSON DECAYS

We compute the branching fractions of the charged Higgs in the flipped 2HDM by adapting the public FORTRAN code **HDECAY** version 3.3 [29]. **HDECAY** computes the branching fractions and total width of the SM Higgs and the Higgs bosons of the minimal supersymmetric standard model (MSSM), including QCD and some electroweak corrections. We adapt the charged Higgs part of the code to the flipped 2HDM by inserting the appropriate $\tan\beta$ dependence for the fermion couplings according to Eq. 9 and eliminating decays to supersymmetric particles. **HDECAY** includes: (i) charged Higgs decays to leptons at tree level, including final state mass effects; (ii) charged Higgs decays to quarks including full one-loop QCD corrections and using the running quark masses in the Yukawa couplings computed to three loops in QCD and evaluated at the charged Higgs mass; and (iii) off-shell decays to $t\bar{b}$ below threshold. No electroweak or supersymmetric corrections are included. Decays via the weak gauge coupling to $\phi^0 W^+$ (where ϕ^0 is one of the neutral states h^0 , H^0 , or A^0) are generically present; for simplicity we eliminate these decays by taking $M_{H^0} = M_{A^0} = M_{H^+}$ and choosing the h^0 – H^0 mixing angle such that the $H^+ h^0 W^-$ coupling is zero.

The branching fractions of the charged Higgs in the flipped model are shown as a function of M_{H^+} in Figs. 1, 2, 3, and 4 for $\tan\beta = 1, 5, 10$, and 50, respectively. For comparison, the corresponding branching fractions in the Type II model are also shown for $\tan\beta \neq 1$. The most consistent feature in both models is the turn-on of decays to $t\bar{b}$ at the kinematic threshold at $M_{H^+} \simeq 180$ GeV. Above this threshold, decays to $t\bar{b}$ dominate for both the

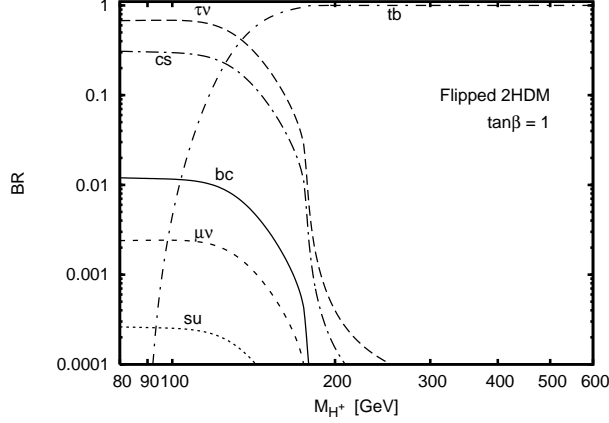


FIG. 1: Charged Higgs branching ratios as a function of M_{H^+} for $\tan\beta = 1$ in the flipped 2HDM. The branching ratios in the Type-II 2HDM are identical.

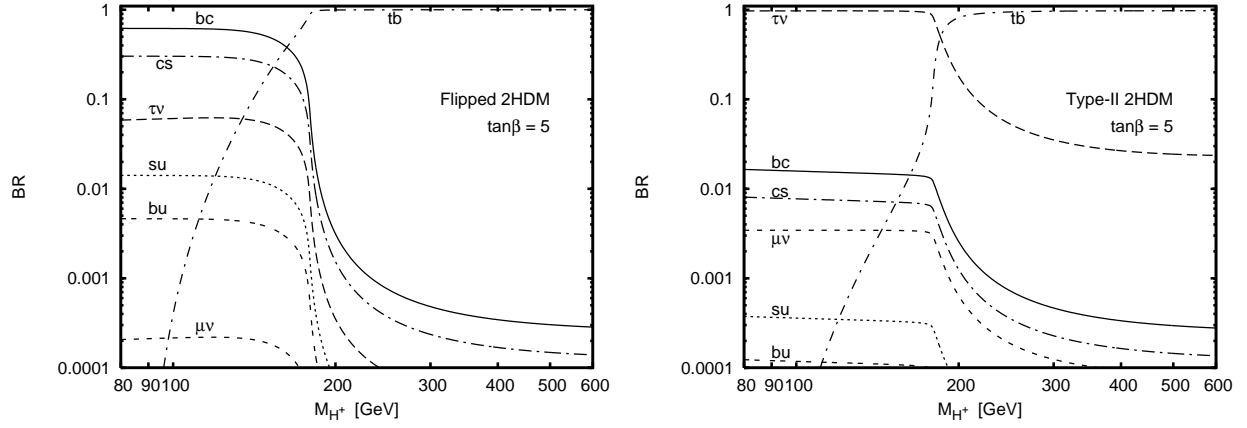


FIG. 2: Charged Higgs branching ratios as a function of M_{H^+} for $\tan\beta = 5$ in the flipped (left) and Type-II (right) 2HDMs.

flipped and Type II models, for all values of $\tan\beta$. As we will see in Sec. IV, this high mass range is favored by the constraint from $b \rightarrow s\gamma$.

Below the $t\bar{b}$ threshold, the effect of the different $\tan\beta$ dependence of the lepton couplings in the flipped and Type II models becomes apparent. We show the branching fractions as a function of $\tan\beta$ in Fig. 5 for $M_{H^+} = 80$ and 130 GeV, for both the flipped and Type-II models. For $\tan\beta = 1$ (Fig. 1), the branching fractions of H^+ in the flipped model are identical to those in the Type-II model. As $\tan\beta$ increases, the branching fraction to $\tau\nu$ is suppressed in the flipped model due to the $\cot\beta$ dependence of the lepton Yukawa couplings. For $\tan\beta = 5$ (Fig. 2), decays to $\tau\nu$ reach at most $\sim 5\%$ in the flipped model, while they dominate below the $t\bar{b}$ threshold in the Type II model. For $\tan\beta = 50$, the branching

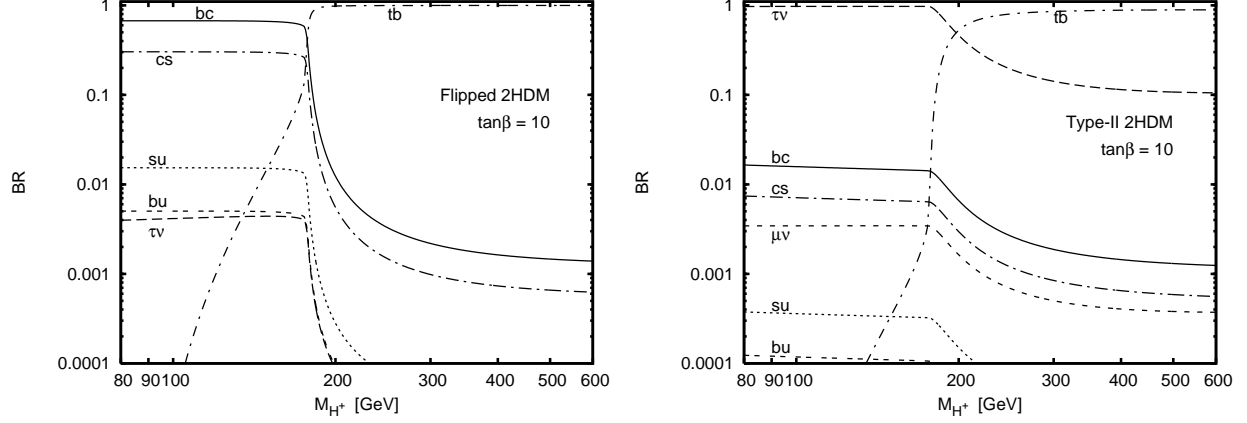


FIG. 3: As in Fig. 2 but for $\tan \beta = 10$.

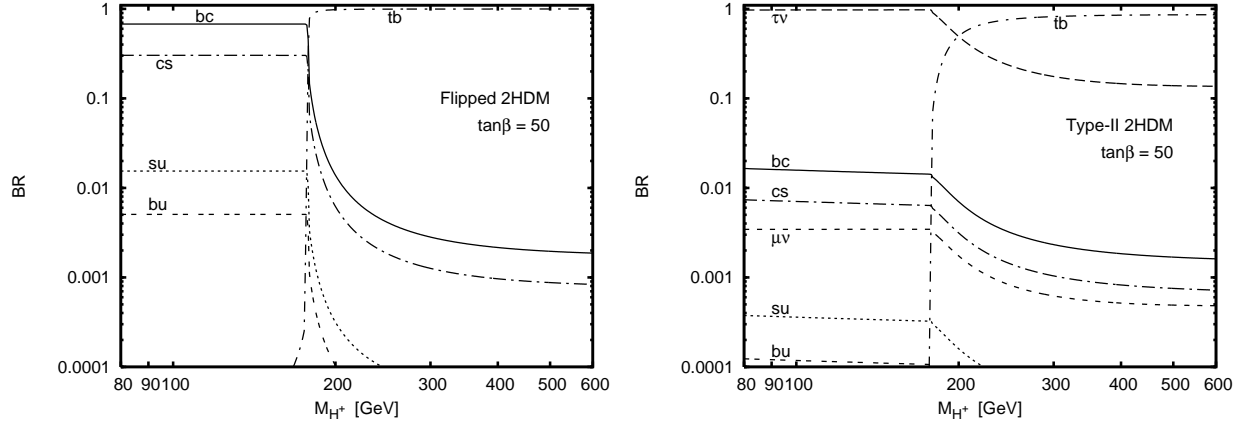


FIG. 4: As in Fig. 2 but for $\tan \beta = 50$.

fraction to leptons is below 10^{-4} . Instead, the dominant decay mode of H^+ for $\tan \beta \gtrsim 3$ is into $c\bar{b}$ with a branching fraction of about $2/3$, followed by $c\bar{s}$ with a branching fraction of about $1/3$. The relative strength of these two decays at moderate to large $\tan \beta$ is controlled by the ratio $V_{cb}m_b/V_{cs}m_s > 1$ (note that in the flipped model the $c\bar{s}$ branching fraction inherits the large uncertainty in the strange quark mass). The dominance of the $c\bar{b}$ mode is in contrast to the Type-II 2HDM; in that model decays to quarks dominate only at low $\tan \beta \lesssim 1$ where the charm quark Yukawa coupling contributes significantly to the rate, leading to $\text{BR}(H^+ \rightarrow c\bar{b})/\text{BR}(H^+ \rightarrow c\bar{s}) \ll 1$.

The total width of the charged Higgs in the flipped and Type-II models is shown in Fig. 6 as a function of M_{H^+} for various $\tan \beta$ values. At $\tan \beta = 1$ the Yukawa couplings are identical in the two models; therefore the total widths are the same. Above the tb threshold at $M_{H^+} \simeq 180$ GeV the total widths are again very similar because the quark Yukawa

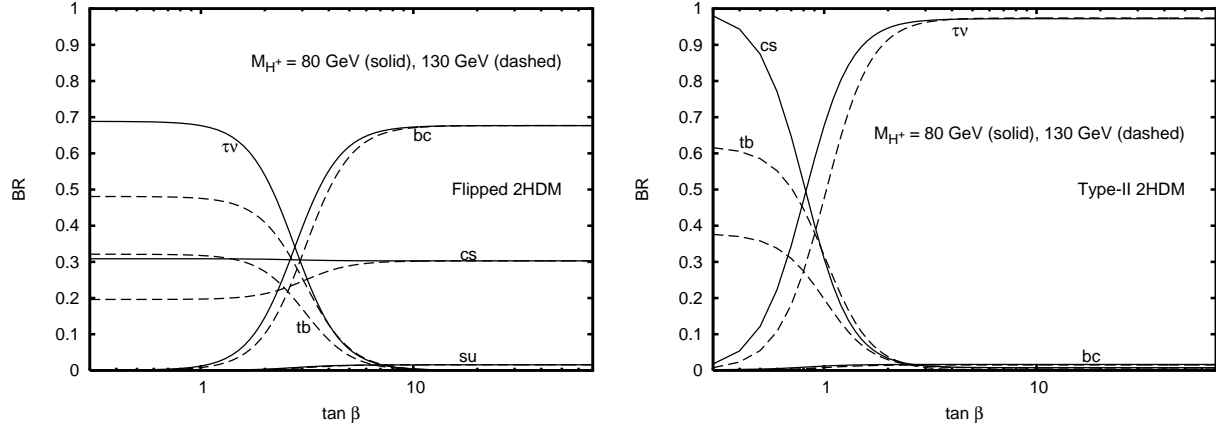


FIG. 5: Charged Higgs branching ratios as a function of $\tan \beta$ for $M_{H^+} = 80$ GeV (solid lines) and 130 GeV (dashed lines) in the flipped (left) and Type-II (right) 2HDMs. Note that off-shell decays to $t\bar{b}$ appear at low $\tan \beta$ as the charged Higgs mass increases.

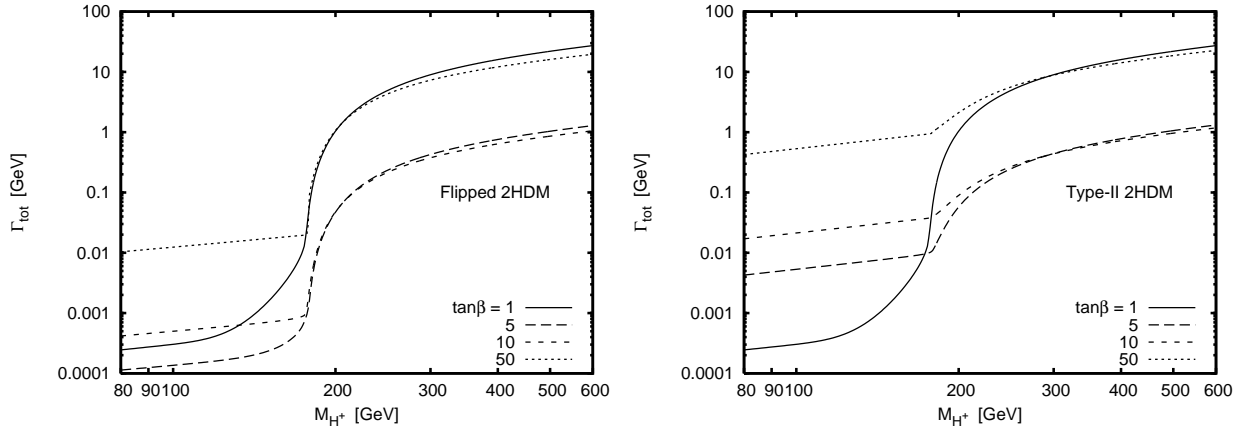


FIG. 6: Total width of the charged Higgs as a function of M_{H^+} , for $\tan \beta = 1, 5, 10$, and 50 , in the flipped (left) and Type-II (right) 2HDMs.

couplings have identical $\tan \beta$ dependence in the two models. Below the $t\bar{b}$ threshold the widths are different in general; in particular, the charged Higgs in the flipped model is much narrower at large $\tan \beta$ because the dominant decays are controlled by couplings proportional to $V_{cb}m_b \tan \beta$ and $V_{cs}m_s \tan \beta$, which are much smaller than the coupling proportional to $m_\tau \tan \beta$ that controls the dominant decay in the Type II model.

IV. INDIRECT CONSTRAINTS

Indirect constraints on the charged Higgs in two-doublet models come from low-energy processes in which an off-shell H^+ is exchanged, either at tree level or at one loop. Tree-level processes include the heavy quark decays $B^+ \rightarrow \tau^+\nu$, $D^+ \rightarrow \tau^+\nu$, and $b \rightarrow c\tau\nu$, in which H^+ exchange can shift the decay branching fraction relative to the SM prediction, as well as decays of the τ lepton in which the ratio of rates to $\mu\nu\bar{\nu}$ versus $e\nu\bar{\nu}$ provides sensitivity to the mass-dependent lepton couplings of H^+ . The former have been used to constrain the Type-II 2HDM [30–33] and the latter to constrain the lepton-specific 2HDM [20, 21]. None of these processes provide constraints in the flipped model, however—the heavy quark decays involve a product of the H^+ couplings to quarks and to leptons, in which the $\tan\beta$ dependence cancels in the flipped model, while the charged Higgs contribution to the τ decay amplitude is proportional to $\cot^2\beta$ which is constrained not to become too large by the perturbativity bound on the top quark Yukawa coupling.

This leaves one-loop processes. The strongest constraint on M_{H^+} in the flipped model comes from the radiative decay $b \rightarrow s\gamma$; low values of $\tan\beta \lesssim 2$ are also constrained by the mass difference ΔM_{B_d} in B^0 – \bar{B}^0 oscillations. The b quark fraction in hadronic Z decays, $R_b \equiv \Gamma(Z \rightarrow b\bar{b})/\Gamma(Z \rightarrow \text{hadrons})$, provides a weaker constraint for $\tan\beta \lesssim 1$. We note however that constraints from one-loop processes are vulnerable to additional new physics that can interfere destructively with the charged Higgs contribution, potentially reopening apparently-excluded parts of parameter space.

A. $b \rightarrow s\gamma$

The strongest indirect constraint on the charged Higgs mass in the flipped 2HDM comes from the process $b \rightarrow s\gamma$. In the SM, this process proceeds through one-loop diagrams involving a W boson and top quark. In models with a second Higgs doublet there are additional diagrams in which the W is replaced by a charged Higgs. Because the charged Higgs contribution to $b \rightarrow s\gamma$ depends only on the charged Higgs couplings to quarks, the constraints in the flipped 2HDM are identical to those in the Type-II model, which have been thoroughly studied.

The measured rate for $b \rightarrow s\gamma$ yields a lower bound on M_{H^+} which is almost independent

of $\tan\beta$ for $\tan\beta \gtrsim 2$; for smaller values of $\tan\beta$ the bound becomes stronger. Because the allowed charged Higgs contribution is quite small, the bound is very sensitive to the experimental central value and the theoretical calculation for the SM rate. The current state-of-the-art theoretical calculation includes QCD corrections at next-to-next-to-leading order [34] for the SM part and next-to-leading order for the charged Higgs part. Using the world average experimental measurement from Ref. [35], combining all theoretical and experimental errors in quadrature, and requiring that $\text{BR}(b \rightarrow s\gamma)$ lie within its 95% (99%) confidence level (CL) bound (a one-degree-of-freedom constraint) yields a lower bound on M_{H^+} of about 295 (230) GeV [34] for $\tan\beta \gtrsim 2$. A separate analysis [36] treating M_{H^+} and $\tan\beta$ as two separate degrees of freedom in a chi-squared fit (a two-degree-of-freedom constraint) found $M_{H^+} \gtrsim 220$ GeV at 95% CL.

B. ΔM_{B_d} and R_b

The mass difference ΔM_{B_d} measured in B^0 – \bar{B}^0 oscillations arises in the SM from box diagrams involving internal W bosons and top quarks. In two-doublet models, diagrams in which one or both of the W bosons is replaced by a charged Higgs give rise to additional contributions that grow with the top quark Yukawa coupling, yielding a lower bound on $\tan\beta$ as a function of the charged Higgs mass [37]. Again, because these contributions depend only on the charged Higgs coupling to quarks, the constraints in the flipped 2HDM are identical to those in the Type-II model. Constraints from this process have been studied recently in Ref. [38], which found $\tan\beta \gtrsim 2.0$ (1.3, 0.9) for $M_{H^+} = 100$ (250, 500) GeV at 95% CL (two-sided one-degree-of-freedom constraint).

The decay $Z \rightarrow b\bar{b}$ receives corrections in two-Higgs-doublet models from loops involving H^+ and top quarks and from loops involving neutral Higgs bosons and bottom quarks [39]. The former are important at low $\tan\beta$ when the top quark Yukawa coupling is enhanced. The latter are important only at high $\tan\beta$ and can be neglected for our purposes. Constraints from this process were studied recently for the Type II model in Ref. [36], which found that they exclude low values of $\tan\beta \lesssim 1$ already disfavored by the ΔM_{B_d} constraint.

V. DIRECT SEARCH CONSTRAINTS

We now consider constraints from direct charged Higgs searches performed at LEP and the Tevatron in the context of the Type-II 2HDM, and show how the resulting limits can be adapted to the flipped model. While the Higgs masses currently accessible to direct searches are already disfavored by $b \rightarrow s\gamma$, the direct limits cannot be avoided by introducing additional new physics in the loops.

A. Limits from LEP

The LEP combined limit on charged Higgs pair production [40] is obtained under the assumption that $\text{BR}(H^+ \rightarrow \tau\nu) + \text{BR}(H^+ \rightarrow c\bar{s}) = 1$. While valid in the Type-II 2HDM, this assumption does not hold in the flipped model; in particular, $H^+ \rightarrow c\bar{b}$ is the dominant decay for $\tan\beta \gtrsim 3$ for charged Higgs masses relevant to the LEP search. This matters because the charged Higgs search at DELPHI [41] actively selected for the $c\bar{s}$ mode, rejecting b jets using the charm mass and decay multiplicity.

In contrast, the searches at ALEPH [42], L3 [43], and OPAL [44] were insensitive to the final-state quark flavor and assumed only that $\text{BR}(H^+ \rightarrow \tau\nu) + \text{BR}(H^+ \rightarrow q\bar{q}) = 1$, which is valid in the flipped model. The most stringent 95% CL limit over most of the parameter space comes from ALEPH, with a slightly stronger limit from OPAL at low $\tan\beta$ where the charged Higgs decay to $\tau\nu$ dominates. The limits are [42, 44],

$$M_{H^+} \geq \begin{cases} 79.3 \text{ GeV} & \text{overall (ALEPH)} \\ 80.4 \text{ GeV} & \text{for } \text{BR}(H^+ \rightarrow q\bar{q}) = 1 \text{ (ALEPH)} \\ 83.0 \text{ GeV} & \text{for } \text{BR}(H^+ \rightarrow \tau\nu) = 0.7 \text{ (OPAL).} \end{cases} \quad (12)$$

Note that for charged Higgs masses around 80 GeV, the branching fraction to $\tau\nu$ never rises above 0.7 in the flipped model (see Fig. 5). These limits are shown in Fig. 7 along with constraints from the Tevatron, which we discuss next.

B. Limits from the Tevatron

The Tevatron experiments CDF and DØ have searched for charged Higgs bosons produced in top quark decay (i.e., for $M_{H^+} < m_t - m_b$) with H^+ decaying to $c\bar{s}$ or $\tau\nu$ [45, 46]. Limits

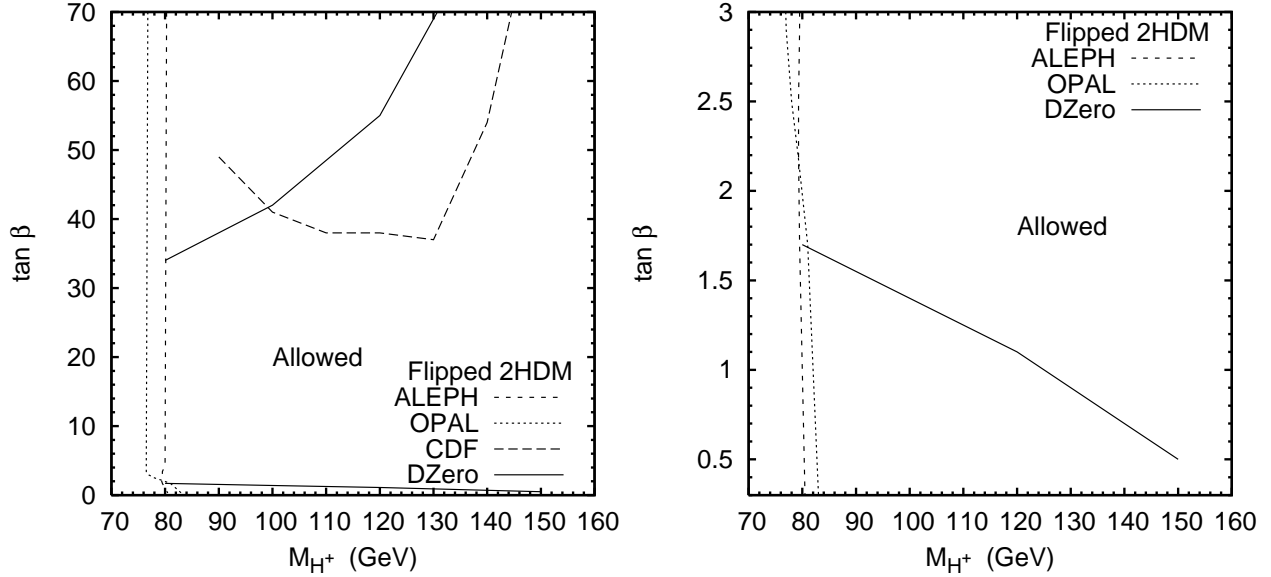


FIG. 7: Direct search limits on the charged Higgs mass and $\tan\beta$ in the flipped 2HDM. ALEPH excludes $M_{H^+} < 80$ GeV over most of the $\tan\beta$ range, with a slightly stronger constraint from OPAL at low $\tan\beta$ where charged Higgs decays to $\tau\nu$ become significant. Large and small values of $\tan\beta$ are excluded by searches at CDF and DØ for charged Higgs production in top quark decay. The plot on the right shows a close-up view of the low $\tan\beta$ region.

from these searches on M_{H^+} and $\tan\beta$ have been presented in the context of the Type-II 2HDM. While the partial width for $t \rightarrow H^+b$ is the same in the flipped and Type-II models, the decay branching fractions for H^+ depend differently on $\tan\beta$, leading to different limits in the flipped model which we derive here.

CDF [45] searched for charged Higgs bosons decaying to $c\bar{s}$ in $t\bar{t}$ events by looking for a second resonance (in addition to the resonance from $W \rightarrow jj$) in the invariant mass distribution of two jets in the lepton-plus-jets $t\bar{t}$ sample. Nonobservation of a second resonance allowed CDF to set a limit on $\text{BR}(t \rightarrow H^+b)$ as a function of M_{H^+} , assuming that $\text{BR}(H^+ \rightarrow c\bar{s}) = 1$. Limits on $\text{BR}(t \rightarrow H^+b)$ are in the range 0.08–0.32 for M_{H^+} between 90 and 150 GeV. No limit is set for M_{H^+} between 70 and 90 GeV due to overwhelming background from the W mass peak.

In the flipped 2HDM, $\text{BR}(H^+ \rightarrow q\bar{q}') \simeq 1$ at large $\tan\beta$, with decays predominantly to $c\bar{b}$. The only difference in the reconstruction of the charged Higgs in this case should be a minor degradation of the energy resolution of the H^+ mass peak due to the poorer energy resolution of bottom quark jets; we expect that this should not significantly reduce the

sensitivity. We apply the CDF constraint to the flipped 2HDM at large $\tan\beta$ by computing $\text{BR}(t \rightarrow H^+b)$ at tree level as a function of M_{H^+} and $\tan\beta$ and taking $\text{BR}(H^+ \rightarrow q\bar{q}') = 1$ (see the Appendix for details). This yields an upper bound on $\tan\beta$ in the range of 40–50 for M_{H^+} between 90 and 140 GeV, as shown in Fig. 7.

DØ [46] searched for charged Higgs production in top quark decays through a fit of the event rates in several single-lepton and two-lepton top quark channels, using the SM prediction for the $t\bar{t}$ cross section and known W decay branching ratios. Charged Higgs production with decays to $q\bar{q}'$ would lead to an overall decrease in the rates for leptonic channels, while charged Higgs production with decays to $\tau\nu$ would increase rates in the hadronic tau channel while decreasing other channels. This allows an upper limit on $\text{BR}(t \rightarrow H^+b)$ of about 0.2 to be set largely independent of the charged Higgs mass. Limits were obtained as a function of $\text{BR}(H^+ \rightarrow q\bar{q}')$ under the assumption that the charged Higgs decays only to $q\bar{q}'$ and $\tau\nu$.

We apply the DØ limits to the flipped 2HDM as follows. At large $\tan\beta$ we take $\text{BR}(H^+ \rightarrow q\bar{q}') = 1$ and compute $\text{BR}(t \rightarrow H^+b)$ at tree level as a function of M_{H^+} and $\tan\beta$. The resulting constraint is weaker than that from the CDF direct search except for $M_{H^+} \simeq 80$ –100 GeV, where the CDF search is degraded by W background; the resulting upper limit on $\tan\beta$ is 34–42. At low $\tan\beta$ we compute the branching fraction of $H^+ \rightarrow q\bar{q}'$ using our modified version of `HDECAY` and translate the appropriate upper limit on $\text{BR}(t \rightarrow H^+b)$ into a lower limit on $\tan\beta$. The resulting limit ranges from 1.7 for $M_{H^+} = 80$ GeV to 0.5 at $M_{H^+} = 150$ GeV. Results for both large and small $\tan\beta$ are shown in Fig. 7.

VI. LHC SEARCH PROSPECTS

We now review the existing LHC charged Higgs search studies and discuss their implications for the flipped 2HDM. Existing ATLAS and CMS studies focus on charged Higgs production via the $H^+\bar{t}b$ coupling: in particular, $t\bar{t}$ production with $t \rightarrow H^+b$ and tH^\pm associated production. Because the quark coupling structure in the flipped model is identical to that in the usual Type-II 2HDM, the charged Higgs production cross sections in these modes are identical in the two models. Likewise, for $M_{H^+} \gtrsim m_t + m_b$, decays of H^+ are predominantly to $t\bar{b}$ in either model. The flipped model phenomenology differs from that of the Type-II model for charged Higgs masses below the $t\bar{b}$ threshold, where decays

of $H^+ \rightarrow q\bar{q}'$ dominate for $\tan\beta$ greater than a few, and above the $t\bar{b}$ threshold insofar as decays to $\tau\nu$ are always completely negligible.

For completeness, we also discuss H^+H^- pair production through electroweak and Yukawa interactions and H^+W^- associated production through Yukawa interactions.

A. $t \rightarrow H^+b$

ATLAS [47] and CMS [48] have studied $t\bar{t}$ production with one top quark decaying to a charged Higgs, $t \rightarrow H^+b$; however, all such studies to date have assumed the charged Higgs decay $H^+ \rightarrow \tau\nu$. While this mode provides good parameter space coverage in the Type-II 2HDM, its range of applicability in the flipped 2HDM is already largely constrained by the $D\bar{D}$ search discussed in the previous section.

Instead, the most relevant search channel in the flipped model would involve the decay $H^+ \rightarrow q\bar{q}'$, as considered already at the Tevatron [45, 46]. We note that the dominant hadronic decay is $H^+ \rightarrow c\bar{b}$; b tagging may thus enhance the signal while at the same time providing evidence for the flipped model Yukawa structure.

B. $H^\pm t$ associated production

The charged Higgs boson can be produced in association with a top quark through bottom-gluon fusion, $gb \rightarrow tH^-$, and through gluon-gluon fusion, $gg \rightarrow \bar{b}tH^-$. The inclusive cross section has been computed to next-to-leading order in QCD [49]. The cross section grows at large $\tan\beta$ proportional to $(m_b \tan\beta)^2$; for $M_{H^+} = 250$ GeV and $\tan\beta = 30$ it reaches about 500 fb [49]. Above the $t\bar{b}$ threshold, the charged Higgs in the flipped 2HDM decays almost exclusively to $t\bar{b}$. Studies of this channel done in the context of the Type-II model can thus be directly applied to the flipped model.

ATLAS [47] and CMS [50] have studied the channel tH^- , $H^- \rightarrow \bar{t}b$ in the context of the MSSM. The charged Higgs production cross section in these studies is identical to that in the flipped model, up to $\tan\beta$ -enhanced corrections to the bottom quark Yukawa coupling from loops involving supersymmetric particles which can affect the tH^- associated production cross section at large $\tan\beta$ [49]. We ignore these corrections here. The major background comes from $t\bar{t}$ plus jets. Unfortunately, both experiments conclude that given the systematic

Cross sections in fb for $M_{H^+} = 200$ GeV					
Process	$\tan \beta = 10$	20	30	50	Source
$q\bar{q} \rightarrow H^+ H^-$	26 for all $\tan \beta$				[51]
$b\bar{b} \rightarrow H^+ H^-$	0.1	0.1	0.5	6	[51]
$gg \rightarrow H^+ H^-$	0.2	2	10	70	[51]
$qq \rightarrow qqH^+ H^-$	17 for all $\tan \beta$				[21, 52]

TABLE II: Charged Higgs pair production cross sections in various modes at the LHC.

uncertainty on the background, this channel yields no discovery potential for $\tan \beta$ values below 100 with 30 fb^{-1} of integrated luminosity. ATLAS combines this tH^- , $H^- \rightarrow \bar{t}b$ channel with tH^- , $H^- \rightarrow \tau\nu$ in the MSSM to present combined discovery reach contours at large $\tan \beta$, but the $H^- \rightarrow \bar{t}b$ contribution improves the reach only marginally [47]. We emphasize that while $\text{BR}(H^- \rightarrow \tau\nu) \sim 10\%$ above the tb threshold in the MSSM at large $\tan \beta$, in the flipped model this decay mode is completely negligible at large $\tan \beta$.

C. $H^+ H^-$ pair production

Charged Higgs bosons can be pair produced via electroweak interactions (Drell-Yan $q\bar{q} \rightarrow \gamma^*, Z^* \rightarrow H^+ H^-$ and weak boson fusion $qq \rightarrow qqH^+ H^-$) and via Yukawa interactions (bottom quark fusion through t -channel top quark exchange, $b\bar{b} \rightarrow H^+ H^-$, and gluon fusion through a one-loop process involving bottom and top quarks in the loop, $gg \rightarrow H^+ H^-$; diagrams involving s -channel exchange of the neutral scalars h^0 and H^0 also contribute). Cross sections in these modes in the flipped model are identical to those in the Type-II 2HDM; representative cross sections are quoted in Table II for $M_{H^+} = 200$ GeV.

The Drell-Yan process and the two Yukawa processes were studied in detail at NLO in Ref. [51]. At low to moderate $\tan \beta$ values, the Drell-Yan process dominates with a cross section of about 26 fb for $M_{H^+} = 200$ GeV. The Yukawa processes are enhanced at large $\tan \beta$, with cross sections growing like $(m_b \tan \beta)^4$; the gluon fusion process dominates at large $\tan \beta$ values, reaching ~ 70 fb at $\tan \beta = 50$.

The weak boson fusion process was studied in detail in Ref. [52]. It does not depend significantly on $\tan \beta$; for $M_{H^+} = 200$ GeV we found a tree-level cross section at the LHC

of 17 fb [21]. While this cross section is rather small, it falls more slowly with increasing M_{H^+} than the s -channel processes and the two forward jets may provide useful kinematic handles against QCD backgrounds.

For charged Higgs masses below the tb threshold, the dominant decay for $\tan\beta$ larger than a few is $H^+ \rightarrow c\bar{b}$, leading to a signal in these channels of $c\bar{b}c\bar{b}$. We expect that this will be completely swamped by four-jet QCD backgrounds. Charged Higgs production in top quark decay has already proven to be a more sensitive channel at the Tevatron and we expect that this will remain true at the LHC.

For charged Higgs masses above the tb threshold, the signal in any of these channels will be $H^+H^- \rightarrow t\bar{t}b\bar{b}$. We expect that backgrounds will be dominated by $t\bar{t}$ just as in the case of the tH^- , $H^- \rightarrow \bar{t}b$ channel discussed in the previous section; at the same time the signal cross section is at least an order of magnitude smaller than for tH^- . Unless the forward jets in the weak boson fusion process can be used to severely reduce the background, we thus expect that these channels will be even less sensitive than tH^- associated production.

D. $H^\pm W^\mp$ associated production

Finally, we consider associated production of a charged Higgs boson with a W^\pm , initiated by $b\bar{b}$ fusion at tree level or gluon fusion at one loop. These processes can proceed directly via H^+ couplings to an initial or internal fermion, as well as via H^+W^- coupling to an s -channel neutral Higgs boson (h^0 , H^0 , or A^0). The leading-order cross sections were computed in Ref. [53] for the MSSM Higgs sector. Cross sections in the flipped 2HDM are the same except for the absence of supersymmetric $\tan\beta$ -enhanced one-loop corrections to the bottom quark Yukawa coupling. We note also that in the MSSM, there are stringent relations among the neutral and charged Higgs boson masses which are absent in a generic 2HDM.

For $M_{H^+} = 200$ GeV, Ref. [53] found

$$\left. \begin{aligned} \sigma(b\bar{b} \rightarrow H^\pm W^\mp) &= 200 \text{ (25, 300) fb} \\ \sigma(gg \rightarrow H^\pm W^\mp) &= 80 \text{ (5, 5) fb} \end{aligned} \right\} \quad \text{for } \tan\beta = 1.5 \text{ (6, 30)}. \quad (13)$$

The $b\bar{b}$ fusion process is dominant, in part because of destructive interference between box and triangle diagrams in the gluon fusion process [53].

Reference [54] studied the LHC search prospects in this channel with $W^\mp \rightarrow \ell\nu$ and $H^\pm \rightarrow tb$; unfortunately, the signal appears to be swamped by the large $t\bar{t}$ background.

VII. CONCLUSIONS

Experimental evidence for a charged Higgs boson would constitute conclusive proof of physics beyond the SM and shed light on the mechanism of electroweak symmetry breaking. The simplest extensions of the SM that contain a charged Higgs are two-Higgs-doublet models. There are four possible assignments of the fermion couplings in two-Higgs-doublet models that naturally avoid tree-level flavor-changing neutral Higgs interactions. The phenomenology and LHC search prospects for the charged Higgs boson in the Type-I and -II models have been studied extensively in the literature; recent papers have done the same for the lepton-specific 2HDM. We complete the picture here by studying the charged Higgs of the flipped 2HDM, in which one doublet gives mass to up-type quarks and charged leptons and the other gives mass to down-type quarks.

The phenomenology of the charged Higgs is controlled by the structure of the Yukawa couplings to quarks and leptons, the charged Higgs mass, and the parameter $\tan\beta$. In the flipped model, the charged Higgs couplings to quarks have the same $\tan\beta$ dependence as in the usual Type-II model. This allowed us to carry over directly from the Type-II model those indirect constraints and charged Higgs production cross sections that depend only on quark couplings. In contrast, the charged Higgs couplings to leptons have the opposite $\tan\beta$ dependence in the flipped model than in the Type-II model. This eliminates indirect constraints from (semi-)leptonic meson decays and leads to a different pattern of charged Higgs decays below the $t\bar{b}$ threshold compared to the Type-II model.

We used these features to extract the existing indirect and direct constraints on the charged Higgs in the flipped model and to evaluate the search prospects at the LHC. The strongest indirect constraint comes from $b \rightarrow s\gamma$, which yields $M_{H^+} \gtrsim 220\text{--}300$ GeV; $B^0\text{--}\bar{B}^0$ mixing also constrains $\tan\beta \gtrsim 2.0$ (1.3, 0.9) for $M_{H^+} = 100$ (200, 300) GeV. Because indirect constraints are vulnerable to contributions from other unknown new physics, we also considered direct search constraints on the charged Higgs from LEP and the Tevatron. Taking account of the different decay patterns in the flipped model compared to the Type-II model, we found that the LEP experiments yield $M_{H^+} \gtrsim 80$ GeV while Tevatron searches for $t \rightarrow H^+b$ put an upper bound on $\tan\beta$ of about 40 for $M_{H^+} \lesssim 130$ GeV and exclude very small $\tan\beta$ values below about 0.5–1.5.

It should be possible at the LHC to extend the Tevatron's sensitivity in $t \rightarrow H^+b$ to

more moderate $\tan \beta$ values, but existing studies consider only the $H^+ \rightarrow \tau \nu$ channel, which would provide sensitivity in the flipped model only at low $\tan \beta$. We expect that the LHC studies could be fruitfully extended to include $H^+ \rightarrow q \bar{q}'$ as in the Tevatron searches.

For charged Higgs masses above the tb threshold, the only potentially promising channel appears to be tH^- associated production with $H^- \rightarrow tb$. Signal rates in the flipped and Type-II models are essentially identical. Unfortunately the most up-to-date ATLAS and CMS studies of this channel with 30 fb^{-1} conclude that the signal is obscured by the systematic uncertainty in the $t\bar{t}$ background. Charged Higgs searches thus remain a major challenge for the LHC.

Acknowledgments

This work was supported by the Natural Sciences and Engineering Research Council of Canada.

Appendix A: Charged Higgs production in top quark decay

We compute the top quark branching fractions as follows. Neglecting the bottom quark mass, the SM partial width for $t \rightarrow W^+ b$ is given at tree level by,

$$\Gamma(t \rightarrow W^+ b) = \frac{G_F m_t}{8\sqrt{2}\pi} [m_t^2 + 2M_W^2] \left[1 - \frac{M_W^2}{m_t^2} \right]^2. \quad (\text{A1})$$

Taking $m_t = 171.2 \text{ GeV}$ and $M_W = 80.398 \text{ GeV}$ [28] yields $\Gamma(t \rightarrow W^+ b) = 1.44 \text{ GeV}$.

In the flipped and Type-II models, the partial width for $t \rightarrow H^+ b$ is given at tree level by,

$$\Gamma(t \rightarrow H^+ b) = \frac{G_F m_t}{8\sqrt{2}\pi} [m_t^2 \cot^2 \beta + m_b^2 \tan^2 \beta] \left[1 - \frac{M_{H^+}^2}{m_t^2} \right]^2, \quad (\text{A2})$$

where we again neglect the final-state bottom quark mass in the kinematics, but keep m_b where it enters the charged Higgs Yukawa coupling. In particular, the decay width becomes large at both low and high $\tan \beta$.

At high $\tan \beta$ the $H^+ \bar{t} b$ coupling is dominated by the term proportional to $m_b \tan \beta$. This coupling receives large QCD corrections, which can be mostly accounted for by using the running bottom quark mass evaluated at the energy scale of the process, which we take to

be M_{H^+} . We use the one-loop expression for the running bottom quark mass,

$$\bar{m}_b(M_{H^+}) = \left[\frac{\alpha_s(M_{H^+})}{\alpha_s(M_b)} \right]^{4/b_0} \bar{m}_b(M_b), \quad (\text{A3})$$

where $b_0 = 11 - 2n_f/3$ and $n_f = 5$ is the number of active quark flavors in the energy range of interest. Here $\bar{m}_b(M_b) = 4.20 \pm 0.04$ GeV [55] is the running bottom quark mass in the modified minimal subtraction scheme evaluated at the bottom quark mass scale, and the running strong coupling α_s is given at one loop by

$$\alpha_s(Q) = \frac{\alpha_s(M_Z)}{1 + (b_0 \alpha_s(M_Z)/2\pi) \ln(Q/M_Z)}. \quad (\text{A4})$$

We use $\alpha_s(M_Z) = 0.1176$ [28].

-
- [1] S. L. Glashow, Nucl. Phys. **22**, 579 (1961); S. Weinberg, Phys. Rev. Lett. **19**, 1264 (1967); A. Salam, in *Elementary Particle Theory, Proceedings Of The Nobel Symposium Held 1968 At Lerum, Sweden*, ed. N. Svartholm (Almqvist and Wiksells, Stockholm, 1969), p. 367.
 - [2] P. W. Higgs, Phys. Rev. Lett. **13**, 508 (1964).
 - [3] S. L. Glashow and S. Weinberg, Phys. Rev. D **15**, 1958 (1977); E. A. Paschos, Phys. Rev. D **15**, 1966 (1977).
 - [4] T. P. Cheng and M. Sher, Phys. Rev. D **35**, 3484 (1987); M. Sher and Y. Yuan, Phys. Rev. D **44**, 1461 (1991); A. Antaramian, L. J. Hall and A. Rasin, Phys. Rev. Lett. **69**, 1871 (1992) [arXiv:hep-ph/9206205].
 - [5] D. Atwood, L. Reina and A. Soni, Phys. Rev. D **55**, 3156 (1997) [arXiv:hep-ph/9609279].
 - [6] S. Davidson and H. E. Haber, Phys. Rev. D **72**, 035004 (2005) [Erratum-ibid. D **72**, 099902 (2005)] [arXiv:hep-ph/0504050].
 - [7] H. E. Haber and D. O'Neil, Phys. Rev. D **74**, 015018 (2006) [arXiv:hep-ph/0602242].
 - [8] R. S. Chivukula and H. Georgi, Phys. Lett. B **188**, 99 (1987); G. D'Ambrosio, G. F. Giudice, G. Isidori and A. Strumia, Nucl. Phys. B **645**, 155 (2002) [arXiv:hep-ph/0207036]; A. V. Manohar and M. B. Wise, Phys. Rev. D **74**, 035009 (2006) [arXiv:hep-ph/0606172].
 - [9] R. M. Barnett, G. Senjanovic, L. Wolfenstein and D. Wyler, Phys. Lett. B **136**, 191 (1984).
 - [10] R. M. Barnett, G. Senjanovic and D. Wyler, Phys. Rev. D **30**, 1529 (1984).
 - [11] T. D. Lee, Phys. Rev. D **8**, 1226 (1973).

- [12] P. Fayet, Nucl. Phys. B **78**, 14 (1974).
- [13] P. Fayet and S. Ferrara, Phys. Rept. **32**, 249 (1977).
- [14] R. D. Peccei and H. R. Quinn, Phys. Rev. Lett. **38**, 1440 (1977).
- [15] H. Georgi, Hadronic J. **1**, 1227 (1978).
- [16] H. E. Haber, G. L. Kane and T. Sterling, Nucl. Phys. B **161**, 493 (1979).
- [17] M. Aoki, S. Kanemura and O. Seto, Phys. Rev. Lett. **102**, 051805 (2009) [arXiv:0807.0361 [hep-ph]]; M. Aoki, S. Kanemura and O. Seto, Phys. Rev. D **80**, 033007 (2009) [arXiv:0904.3829 [hep-ph]].
- [18] H. S. Goh, L. J. Hall and P. Kumar, JHEP **0905**, 097 (2009) [arXiv:0902.0814 [hep-ph]].
- [19] S. Su and B. Thomas, Phys. Rev. D **79**, 095014 (2009) [arXiv:0903.0667 [hep-ph]].
- [20] M. Aoki, S. Kanemura, K. Tsumura and K. Yagyu, Phys. Rev. D **80**, 015017 (2009) [arXiv:0902.4665 [hep-ph]].
- [21] H. E. Logan and D. MacLennan, Phys. Rev. D **79**, 115022 (2009) [arXiv:0903.2246 [hep-ph]].
- [22] V. D. Barger, J. L. Hewett and R. J. N. Phillips, Phys. Rev. D **41**, 3421 (1990).
- [23] Y. Grossman, Nucl. Phys. B **426**, 355 (1994) [arXiv:hep-ph/9401311].
- [24] V. Barger, H. E. Logan and G. Shaughnessy, Phys. Rev. D **79**, 115018 (2009) [arXiv:0902.0170 [hep-ph]].
- [25] A. G. Akeroyd and W. J. Stirling, Nucl. Phys. B **447**, 3 (1995); A. G. Akeroyd, Phys. Lett. B **377**, 95 (1996) [arXiv:hep-ph/9603445]; Nucl. Phys. B **544**, 557 (1999) [arXiv:hep-ph/9806337].
- [26] A. G. Akeroyd, J. Phys. G **24**, 1983 (1998) [arXiv:hep-ph/9803324].
- [27] J. F. Gunion, H. E. Haber, G. L. Kane, and S. Dawson, *The Higgs Hunter's Guide* (Westview Press, Boulder, Colorado, 2000), SCIPP-89/13.
- [28] C. Amsler *et al.* [Particle Data Group], Phys. Lett. B **667**, 1 (2008).
- [29] A. Djouadi, J. Kalinowski and M. Spira, Comput. Phys. Commun. **108**, 56 (1998) [arXiv:hep-ph/9704448].
- [30] W. S. Hou, Phys. Rev. D **48**, 2342 (1993).
- [31] A. G. Akeroyd, C. H. Chen and S. Recksiegel, Phys. Rev. D **77**, 115018 (2008) [arXiv:0803.3517 [hep-ph]].
- [32] Y. Grossman and Z. Ligeti, Phys. Lett. B **332**, 373 (1994) [arXiv:hep-ph/9403376].
- [33] Y. Grossman, H. E. Haber and Y. Nir, Phys. Lett. B **357**, 630 (1995) [arXiv:hep-ph/9507213].

- [34] M. Misiak *et al.*, Phys. Rev. Lett. **98**, 022002 (2007) [arXiv:hep-ph/0609232].
- [35] E. Barberio *et al.* [Heavy Flavor Averaging Group (HFAG)], arXiv:hep-ex/0603003.
- [36] A. Wahab El Kaffas, P. Osland and O. M. Ogreid, Phys. Rev. D **76**, 095001 (2007) [arXiv:0706.2997 [hep-ph]].
- [37] C. Q. Geng and J. N. Ng, Phys. Rev. D **38**, 2857 (1988) [Erratum-ibid. D **41**, 1715 (1990)]; P. Ball and R. Fleischer, Eur. Phys. J. C **48**, 413 (2006) [arXiv:hep-ph/0604249].
- [38] F. Mahmoudi and O. Stal, arXiv:0907.1791 [hep-ph].
- [39] A. Denner, R. J. Guth, W. Hollik and J. H. Kuhn, Z. Phys. C **51**, 695 (1991).
- [40] LEP Higgs Working Group for Higgs boson searches and ALEPH, DELPHI, L3, and OPAL Collaborations, arXiv:hep-ex/0107031.
- [41] J. Abdallah *et al.* [DELPHI Collaboration], Eur. Phys. J. C **34**, 399 (2004) [arXiv:hep-ex/0404012].
- [42] A. Heister *et al.* [ALEPH Collaboration], Phys. Lett. B **543**, 1 (2002) [arXiv:hep-ex/0207054].
- [43] P. Achard *et al.* [L3 Collaboration], Phys. Lett. B **575**, 208 (2003) [arXiv:hep-ex/0309056].
- [44] G. Abbiendi *et al.* [OPAL Collaboration], arXiv:0812.0267 [hep-ex].
- [45] T. Aaltonen *et al.* [CDF Collaboration], Phys. Rev. Lett. **103**, 101803 (2009) [arXiv:0907.1269 [hep-ex]].
- [46] V. M. Abazov *et al.* [D0 Collaboration], Phys. Lett. B **682**, 278 (2009) [arXiv:0908.1811 [hep-ex]].
- [47] G. Aad *et al.* [The ATLAS Collaboration], arXiv:0901.0512 [hep-ex].
- [48] M. Baarmand, M. Hashemi and A. Nikitenko, J. Phys. G **32**, N21 (2006).
- [49] T. Plehn, Phys. Rev. D **67**, 014018 (2003) [arXiv:hep-ph/0206121].
- [50] S. Lowette and J. D'Hondt, CMS Note 2006/109 (2006), available from <http://cdsweb.cern.ch>.
- [51] A. Alves and T. Plehn, Phys. Rev. D **71**, 115014 (2005) [arXiv:hep-ph/0503135].
- [52] S. Moretti, J. Phys. G **28**, 2567 (2002) [arXiv:hep-ph/0102116].
- [53] A. A. Barrientos Bendezu and B. A. Kniehl, Phys. Rev. D **59**, 015009 (1999) [arXiv:hep-ph/9807480].
- [54] S. Moretti and K. Odagiri, Phys. Rev. D **59**, 055008 (1999) [arXiv:hep-ph/9809244].
- [55] O. Buchmuller and H. Flacher, Phys. Rev. D **73**, 073008 (2006) [arXiv:hep-ph/0507253].